ELSEVIER

Biophysical Chemistry 64 (1997) 157–173

Biophysical Chemistry

Tertiary and quaternary chloride effects of the partially ligated (CN-met) hemoglobin intermediates

Yingwen Huang, Mary L. Koestner, Gary K. Ackers *

Department of Biochemistry and Molecular Biophysics, Washington University School of Medicine, Box 8231, St. Louis, MO 63110 USA

Received 16 July 1996; accepted 10 September 1996

Abstract

Heterotropic effects of NaCl were studied using CN-met hemoglobin, which has been found to follow the same rules of homotropic cooperativity as CO-Hb and O_2-Hb [Huang and Ackers, Biochemistry,35 (1996) 704; Huang et al., Biophys. J., 71 (1996) 2094]. Modulation of heme site cooperativity by NaCl was determined in this study for all partially ligated CN-met intermediates by measuring their dimer-to-tetramer assembly free energies as a function of NaCl concentration (0.08–1.4 M; pH 7.4, $T = 21.5$°C). Thermodynamic linkage analysis yielded the contributions to heme site binding cooperativity for all 16 reactions of the binding cascade, and also their apparent changes in bound salt. The principal findings were as follows: (i) At each [NaCl] the ten tetrameric species exhibited three discrete cooperative free energy levels; (ii) positional isomers of the doubly ligated tetramers were distributed among two of these levels according to their specific configurations of ligated sites, in conformity with the symmetry rule mechanism of hemoglobin cooperativity [Ackers et al., Science 255 (1992) 54]; (iii) the apparent moles of NaCl release followed the same configuration-specific distribution as that of heme site cooperativity, i.e., this parameter was synchronized according to the same response clusters. The system thus manifests both a "tertiary chloride effect" and a "quaternary chloride effect", which parallel the tertiary and quaternary Bohr effects [Daugherty et al., Biochemistry, 33 (1994) 10345; Perrella et al., Biochemistry, 33 (1994) 10358] and the tertiary and quaternary enthalpy effects [Huang and Ackers, Biochemistry, 34 (1995) 6316].

Comparison with findings on the stoichiometric O_2-binding linkages over an identical range of conditions [Doyle et al., Biophys. Chem., 64 (1997)] revealed that the overall NaCl release upon ligating all four hemes is identical for O_2 and CN-met, whereas the detailed distributions of apparent chloride release showed variations between the two ligands, i.e., CN-met Hb showed only a negligible quaternary enhancement at all [NaCl] conditions and a larger tertiary chloride effect compared with O_2-Hb. Possible origins of these variations are considered.

Keywords: Allosteric regulation; Cooperativity; Hemoglobin intermediate; Subunit assembly

1. Introduction

Efforts to decipher the rules of cooperative interaction among the four subunits of tetrameric hemoglobin (i.e. a "molecular code" [1,2]) have been limited for decades because experimental O_2 binding isotherms could not distinguish between configurational isomers at the successive stoichiometric degrees of binding. Although accurate measurements at this level of detail continue to provide

* Corresponding author.

PII S0301-4622(96)02236-3

important insights and constraints (cf. 3), contributions from the eight configuration-specific binding intermediates (Fig. 1) have become resolvable during the last several years. Elucidation of the detailed thermodynamics of heme site ligation and its linkages to heterotropic effectors has required circumvention of the following obstacles: (i) lability of the heme iron–oxygen bond precludes the isolation and study of most intermediates; (ii) high binding cooperativity greatly reduces the populations of intermediates in equilibrium with the end-state species; and (iii) dissociation of tetramers into dimers leads to their reassembly into tetramers with rearranged configurations of occupied sites (Fig. 2).

Determination of the contributions to binding cooperativity by each of the partially ligated intermediates has been accomplished by the use of (i) tightly bound oxygen analogs, e.g. CN-met or CO in place of O_2 [1,2,4–6]), or (ii) metal-substituted hemes that mimic the natural system (e.g. replacement of iron by cobalt, manganese, or zinc [7–11]. Resolution of cooperativity properties for all eight intermediates

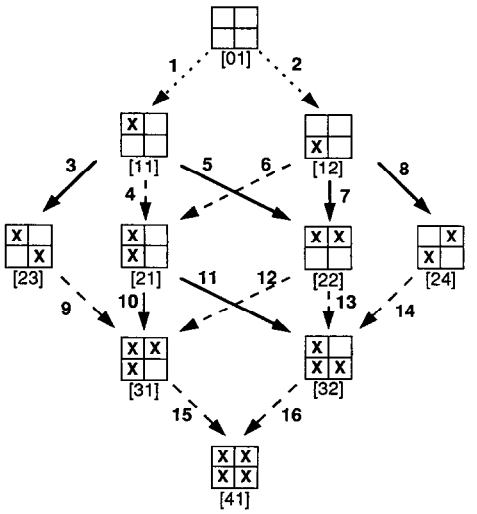

Fig. 1. Topographic representation of the 10 ligation microstates of hemoglobin and the 16 stepwise binding reactions. Relative orientation of subunits within tetramers is indicated in the top species 01. Index ij denotes the particular species j among those with i ligands bound ($i = 0$–4; $j = 1$–4). Ordering with respect to j is arbitrary. Ligated heme sites (x) in this study contain Fe(III)-CN, while Fe(II) hemes are in each unligated (blank) subunit. Dotted, dashed and solid arrows denote stepwise ligation reactions accompanied by tertiary constraint transitions, null transitions and quaternary switch transitions, respectively.

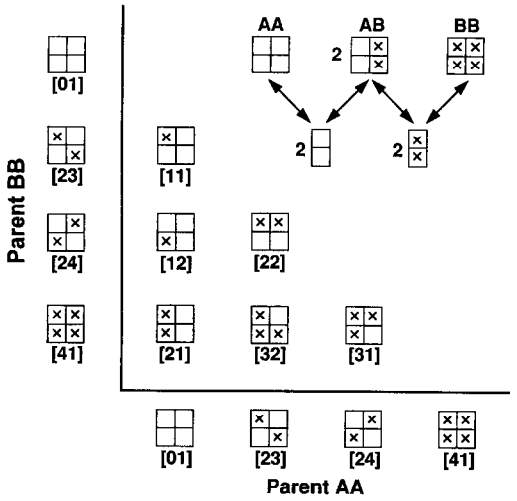

Fig. 2. Hybridization scheme for construction of the six tetrameric species from their parent molecules. Formation of each hybrid like AB from dissociated parent tetramers AA and BB occurs by the dissociation reassociation reactions indicated.

resulted from the extension of a conceptual strategy developed previously for analyzing the linkages between oxygen-binding and subunit assembly [12]. Its application to the site-specific intermediates of Hb [1,2,4,7–11,13,14,16,18] led to a specific "molecular code" [18–20], i.e., a set of rules which translate the 16 changes in site occupancy that may result from ligation (Fig. 1) into six switchpoints of quaternary T → R structure change. The proposed molecular code (also called "symmetry rule mechanism") was derived from: (i) free energy distributions determined for ligation microstates of the first three systems resolved (i.e., $Fe^{2+}/Fe^{3+}CN$, Fe^{2+}/Mn^{3+} and $Co^{2+}/Fe^{2+}CO$) [1], in combination with (ii) structure-sensitive probes that provided quaternary assignments for these tetrameric species [13,18–20], and (iii) O_2-binding and subunit assembly properties of normal Hb and cobalt-substituted Hb [9] that were resolved at the four stoichiometric levels (e.g. [3]). On the basis of these results, a partition function was deduced for the hemoglobin allosteric mechanism [20], which translates the ligand-driven structural

[1] Nomenclature ($M^a_{(i)}/M^b_{(ii)}$) used here to denote analog systems specifies the "unligated" heme site metal $M_{(i)}$ with charge a, in combination with subunits $M^b_{(ii)}$ containing metal ions $M^b_{(ii)}$ that may also be reacted with ligand X.

features of tertiary and quaternary switching into the 16 configuration-specific binding steps of the Hb cascade, Fig. 1 (specific rules of this mechanism are described in Section 2.4. As with enzyme substrate analogs, the mechanistic rules deduced from data on oxygen-binding analogs must be reconciled with properties of the native system, even though the magnitudes of the effects may be expected to differ [2]. Analyses have found that the symmetry rule partition function is also consistent with the four-stage oxygen-binding data of native Hb as a function of pH [14] and temperature [16]. Recently, the detailed cooperativity properties explicitly resolved for the binding intermediates of carbon monoxide and oxygen have also been found to follow the same molecular code as with CN-met ligation [10,11].

In the present study we analyzed the heterotropic effects of NaCl on the free energies of CN-met Hb with all combinations of ligated and unligated heme sites. By model-independent linkage relationships, the dependences on [NaCl] of terms in the Hb partition function have yielded the apparent changes in salt binding for each of the 16 heme site reactions of Fig. 1. These salt linkages for CN-met Hb will be compared with the linkages to oxygenation, determined over the same [NaCl] range at each stoichiometric degree of binding [3]. Results from the two studies are discussed in relation to their implications for the symmetry rule mechanism and to the validity of CN-met Hb as a model for hemoglobin oxygenation.

2. Conceptual framework and background

2.1. Configuration-specific parameters of binding and cooperativity

The free energy of binding i moles of ligand X to form each of the tetrameric microstate species ij from unligated species 01 is characterized by the equilibrium constant k_{ij} = [species ij]/[species 01][X], where brackets denote species concentrations. These configuration-specific binding constants are thermodynamically linked to the equilibrium constants of dimer–tetramer assembly for the ij species of Fig. 1 through each respective linkage cycle [1,2,16] so that

$$ {}^{ij}k_2 / {}^{01}k_2 = k_{ij}/k_\alpha^p k_\beta^q \equiv {}^{ij}k_c \qquad (1) $$

Equilibrium constants ${}^{ij}k_2$ and ${}^{01}k_2$ pertain to the dimer–tetramer assembly reactions of species ij and 01, k_α and k_β are binding constants to the α and β subunits of dissociated dimers, and p and q are the respective numbers of ligated subunits of each kind within the tetramer ij. The configuration-specific coupling constant ${}^{ij}k_c$ equals the binding constant for forming species ij from species 01 when normalized to the appropriate combination of intrinsic binding constants k_α and k_β, each raised to their stoichiometric power p or q. When this ratio is incorporated into the expression $[-RT \ln(k_{ij}/k_\alpha^p k_\beta^q)]$, it is seen to reflect explicitly the free energy cost of reacting ligand species X at i tetrameric sites ($p + q = i$) to form species ij, minus the free energy $[-RT \ln(k_\alpha^p k_\beta^q)]$ of ligating the same sites of dissociated dimers. The "cooperative free energy" is thus: ${}^{ij}\Delta G_c = -RT \ln {}^{ij}k_c$. For practical reasons, the ratio of assembly constants on the left of Eq. (1) often affords the most experimentally feasible approach to determining ${}^{ij}\Delta G_c$. This bypasses the necessity to measure actual ligand affinities in order to assess contributions to cooperativity by the different species [1,2,17], as the assembly data evaluate the energetics of molecular events which accompany heme site binding to the tetrameric molecules by difference from those occurring in the respective dissociated dimers. The first application of this principle to the 10 Hb microstates [1] opened the field to explicit resolution of all site-specific cooperativity contributions for tightly bound (or non-dissociable) oxygen analogs. A set of "cooperative free energies" for the intermediate species provides an assessment of the contributions by each tetrameric species to the cooperativity of binding.

2.2. Relationships to the traditional binding constants

Values of ${}^{ij}\Delta G_c$ for the nine ligated Hb microstates are explicitly related to the four stoichio-

[2] A classic example of this strategy with an allosteric enzyme has been the extensive use of the bisubstrate analog PALA (*N*-phosphonoacetyl-L-aspartate) which, even though completely unreactive, has been found to mimic the natural enzyme–substrate complex of aspartate transcarbamylase [cf. S.R. Wente and H.K. Schachman, Proc. Natl. Acad. Sci. U.S.A., 84 (1987) 31–35].

metric Adair binding constants K_{4i} (i.e. for reacting the deoxy tetramer with i ligands regardless of site configuration) by first noting from Eq. (1) that

$$k_{ij} = k_\alpha^p k_\beta^q \left({}^{ij}k_c\right) \quad (2)$$

When dissociated dimers bind non-cooperatively with a single equilibrium constant k_d, Eq. (2) becomes

$$k_{ij} = (k_d)^i \times {}^{ij}k_c \quad (3)$$

Relationships between the site-specific cooperativity constants ${}^{ij}k_c$ and the classical Adair binding constants K_{4i} are therefore

$$K_{41} = 2(k_{11} + k_{12}) = 2k_\alpha\left({}^{11}k_c\right) + 2k_\beta\left({}^{12}k_c\right) \quad (4)$$

$$\begin{aligned} K_{42} &= 2k_{21} + 2k_{22} + k_{23} + k_{24} \\ &= 2k_\alpha k_\beta\left({}^{21}k_c\right) + 2k_\alpha k_\beta\left({}^{22}k_c\right) \\ &\quad + (k_\alpha)^2\left({}^{23}k_c\right) + (k_\beta)^2\left({}^{24}k_c\right) \end{aligned} \quad (5)$$

$$\begin{aligned} K_{43} &= 2(k_{31} + k_{32}) \\ &= 2(k_\beta)^2 k_\alpha\left({}^{31}k_c\right) + 2(k_\alpha)^2 k_\beta\left({}^{32}k_c\right) \end{aligned} \quad (6)$$

$$K_{44} = k_{44} = (k_\alpha)^2(k_\beta)^2\left({}^{41}k_c\right) \quad (7)$$

The right hand expressions of Eqs. (4)–(7) provide a configuration-specific formulation of terms in the standard binding partition function Z_4 for the four-site tetramer (see [20])

$$Z_4 = 1 + K_{41}(X) + K_{42}(X)^2 + K_{43}(X)^3 + K_{44}(X)^4 \quad (8)$$

Then the tetrameric binding isotherm $\bar{Y}_4$ (i.e., the fraction of heme sites ligated) is

$$\begin{aligned} \bar{Y}_4 &= \frac{1}{4}\frac{d\ln Z_4}{d\ln(X)} \\ &= \frac{K_{41}(X) + 2K_{42}(X)^2 + 3K_{43}(X)^3 + 4K_{44}(X)^4}{4\left[1 + K_{41}(X) + K_{42}(X)^2 + K_{43}(X)^3 + K_{44}(X)^4\right]} \end{aligned} \quad (9)$$

Additional properties of site-specific binding partition functions have been described by Di Cera [21]. It should be noted that conventional binding isotherms, measured as a function of Hb concentration, can be analyzed to obtain the stoichiometric binding constants K_{4i} and their linked stoichiometric constants of dimer–tetramer assembly ${}^{i}K_2$, whereas data of the present study yield the microstate coupling constants ${}^{ij}k_c$ for all the ligation species of Fig. 1. Values of ${}^{ij}k_c$ were determined in this study from the measured ratios $({}^{ij}k_2/{}^{01}k_2)$ with particular interest in comparing the CN-met microstate properties with stoichiometric O_2-binding results over the same [NaCl] range (Section 4.3). Eqs. (1)–(9) provide a basis for those comparisons. Although non-labile O_2 analogs such as CN-met afford resolution of cooperativity parameters at the desired level of all 10 microstates, they cannot be studied solely by direct binding methods. The alternative approach has utilized the linkages to dimer–tetramer assembly (Eq. (1)). It is therefore important that strong evidence for non-cooperativity in CN-met ligation by dissociated Hb dimers has been provided by extensive studies of O_2-binding to the vacant sites of Hb tetramers and dimers that were partially ligated in various combinations with CN-met sites [13].

2.3. Cooperative free energy distributions for the ligation intermediates of hemoglobin

Initial experiments [1] based on the thermodynamic framework of Eqs. (1)–(9) led to the discovery that configurational isomers of heme site ligation can have different cooperativity properties, even with identical numbers of bound ligands (see also [5,6,10,11,13]). Cooperative free energy distributions for the initially resolved O_2-analog systems were found [17] to be incompatible with the concerted allosteric model [23] [3].For each system the four dou-

[3] For example, the concerted MWC model [23] postulates two alternative quaternary structures (T and R) along with the special rule that all subunits in quaternary structure "T" have the same tertiary conformation, whereas they all have a second tertiary conformation in the alternative quaternary form "R". The changing net affinities at successive binding steps is generated solely through a progressively increasing ratio of the high affinity (R) species to those with the low (T) affinity, i.e., this model assumes cooperativity properties that vary with the number of bound ligands, irrespective of site configuration. Critical tests for the concerted model would thus necessitate experimental measurements capable of explicitly resolving cooperativity properties of the configurational isomers at each stoichiometric degree of heme site ligation (Fig. 1). By contrast, the sequential KNF model [24] postulates changes in affinity to arise during the binding sequence from altered near-neighbor subunit interactions as a result of ligand-driven tertiary conformation changes. These divergent mechanisms have been found to represent O_2-binding isotherms with equal accuracy, [24] demonstrating that a unique mechanism cannot be established from ligand saturation curves alone.

bly ligated species (Fig. 1) were partitioned into two levels; species 21 occupied a common level with singly ligated species 11 or 12 (or occupied a level of its own), whereas species 22, 23, 24, 31, and 32 occupied a separate level. Species 41 was either distributed with the triply ligated tetramers or occupied a separate level which indicated quaternary enhancement; i.e., the fully ligated tetramer assembles more favorably from its dimers than the triply ligated species (cf. [3]).

These observations of a similar distribution for the model-independent terms in the partition functions for each of the chemically diverse O_2-analog systems (Fe/FeCN, Fe/Mn^{3+}, and Co/FeCO), and the assumption that this pattern reflected a common mechanism (i.e. where each species *ij* plays a similar role in the various "ligand systems") suggested the following "consensus relationships" between cooperativity parameters ${}^{ij}k_c$

$$ {}^{11}k_c = {}^{12}k_c \equiv K_{tc} \tag{10} $$

$$ {}^{21}k_c \equiv K_{tc}^{21} \tag{11} $$

$$ {}^{22}k_c = {}^{23}k_c = {}^{24}k_c = {}^{31}k_c = {}^{32}k_c \equiv K_c K'_{tc} \tag{12} $$

$$ {}^{41}k_c \equiv K_c \tag{13} $$

Thus each configuration-specific contribution ${}^{ij}k_c$ to the K_{4i} terms of the partition function, Eq. (8), was found to bear a similar relationship to the remaining eight terms in each of the three analog systems. This finding suggested strongly that a specific mechanistic role was therefore encoded by the parameters K_{tc}, K_{tc}^{21}, K'_{tc}, and K_c.

2.4. Symmetry rule mechanism

To interpret the mechanistic significance of Eqs. (10)–(13), it was necessary to relate K_{tc}, K_{tc}^{21}, K'_{tc}, and K_c to structural changes of tertiary and quaternary transition that have long been known to accompany ligation of the heme sites. Studies of the various intermediates using probes of quaternary structure [13–16,18–22] showed that the three "model parameters" occurring singly, or in combinations on the right sides of Eqs. (10)–(12) (along with the model-independent parameter K_c of Eq. (13)). must reflect the energetic contributions to cooperativity by the ligation-induced tertiary and quaternary structural transitions through the cascade of heme site binding (Fig. 1).

The rules deduced for these molecular events from combination of the site-specific thermodynamic results and the quaternary structure probes [20,13] are as follows. (i) Binding the initial ligand induces a tertiary conformational change within both subunits of the dimeric half-molecule ($\alpha^1\beta^1$ or, equivalently, $\alpha^2\beta^2$). This reaction generates opposing free energy of "tertiary constraint" ΔG_{tc} so that the net binding energy is lower than for the sites of dissociated dimers. (ii) Binding a second ligand within the same dimeric half-tetramer generates a reduced (or zero) increment of tertiary constraint so that binding is more favorable. Thus there is cooperativity between the α and β subunits within a dimeric half-tetramer prior to quaternary switching. (iii) Switching from the quaternary T to the quaternary R structure (defined by orientation of the two dimeric half-tetramers $\alpha^1\beta^1$ and $\alpha^2\beta^2$) is promoted by all binding steps where the tetramer acquires at least one ligated site on each dimeric half-molecule. These six $T \rightarrow R$ switchpoints are indicated by the solid arrows in Fig. 1. Quaternary switching is facilitated by unfavorable free energy arising when both dimers within the T tetramer are ligated (dimer–dimer anticooperativity; cf. [20]). The $T \rightarrow R$ switchover releases the stored tertiary constraint energy ΔG_{tc} and globally alters non-covalent bonds of the dimer–dimer interface. As the free energy arising from alteration of interfacial bonds at the quaternary switchover exceeds ΔG_{tc}, an additional gain of cooperative free energy is manifested at each of the six switchpoints.

Quantitative formulation of these mechanistic rules according to the parameters of Eqs. (10)–(13) is as follows: K_c represents the free energy cost of alterations in binding affinity over all four binding steps (the same for any pathway of the cascade); K_{tc} reflects the creation of tertiary constraint upon initial ligation (onto either α or β); K_{tc}^{21} reflects tertiary constraint for ligating both sites on an $\alpha\beta$ half-tetramer prior to quaternary switchover ($T \rightarrow R$); the ratio K_{tc}^{21}/K_{tc} thus reflects cooperativity between the two binding steps that create species 21 (i.e., cooperativity within the half-tetramer prior to switching from the quaternary T structure); finally, the product $K'_{tc} \cdot K_c$ reflects quaternary enhancement when $K'_{tc} > 1$.

By substituting the rightmost terms of Eqs. (10)–

(13) for the coupling constants ${}^{ij}k_c$ of Eqs. (4)–(7), and then substituting the resultant expressions for Adair binding constants K_{4i} of Eq. (8), the binding partition function is expressed in parameters of the symmetry rule mechanism [20,13], i.e.

$$Z_4 = 1 + 2K_{tc}(k_\alpha + k_\beta)X + \left[2k_\alpha k_\beta\left(K_{tc}^{21} + K_c K'_{tc}\right) + \left(k_\alpha^2 + k_\beta^2\right)K_c K'_{tc}\right]X^2 + 2K_c K'_{tc}\left(k_\alpha k_\beta^2 + k_\alpha^2 k_\beta\right)X^3 + k_\alpha^2 k_\beta^2 K_c X^4 \quad (14)$$

The tetrameric binding isotherm may be calculated from the symmetry rule partition function, Eq. (14), by substituting for Z_4 into Eq. (9). Each ligand or ligand analog may be expected to differ in values of the constants [K_α, K_β, K_{tc}, K_{tc}^{21}, K'_{tc} and K_c], while their fixed relationships to the microstate constants (Eqs. (10) and (11)) must hold over the 10 ligation species in order to conform with this mechanism. By this test, the overall oxygen-binding isotherms and carbon monoxide isotherms of hemoglobin have been found to be entirely consistent with the symmetry rule mechanism, while implying physically reasonable values of the model parameters [10,11,13,18,20].

2.5. *Is the symmetry rule mechanism an artifact of CN-met ligation?*

Oxygenation analog systems analyzed subsequently to proposal of the symmetry rule mechanism involving both metal substitution and heme site ligation have been found to have similar combinatorial distributions to Eqs. (10)–(13) with minor variations in spacings of the four energy levels [8,10,11]. It was found that such variations may result from specific metal-substitution effects that can be evaluated and corrected. Thus, the free energies of all 10 microstates of carbon monoxide binding to normal FeHb were recently determined [10] and a similar study with $Zn^{2+}/Fe^{2+}O_2$ species [11] has yielded microstate free energies of the native Hb O_2 system (i.e., $Fe^{2+}/Fe^{2+}O_2$). The model-independent distribution of cooperative free energies for intermediates of O_2-binding thus resolved from studies on zinc/iron hybrid tetramers was found to be identical with that predicted four years earlier [20] from analysis of stoichiometric oxygenation data using Eqs. (4)–(13). These recent findings have provided verification of the deductions originally made from the three ligation systems Fe/FeCN, Fe/Mn^{3+} and Co/FeCO.

An opposite viewpoint has been promoted on the basis of oxygen-binding experiments conducted by Mozzarelli and co-workers [52–54] on hemoglobin samples within crystal lattices. These samples were incapable of cracking upon oxygenation, showed no cooperativity, no Bohr effect, and bound O_2 with extremely reduced affinity compared with the first binding step of solution samples. Because of these compromised functional properties, the data of Mozzarelli and co-workers have been claimed by Eaton [53,54] as proof that quaternary T tetramers are incapable of O_2-binding cooperativity, even in solution. On this basis Eaton has suggested that CN-met ligation should be dismissed as irrelevant to the allosteric mechanism of O_2-binding because CN-met cooperativity does accompany ligation of the quaternary T tetramers of normal Hb in solution [1,2,4]. The following argument has been advocated. (a) Confinement of unligated tetramers within these crystals, which prevent the normal oxygenation-induced tertiary and quaternary structure changes, has produced a population of molecules identical with those of unligated T tetramers in solution. (b) The O_2-binding properties measured on such a crystalline sample should therefore also portray the oxygenation properties of T tetramers in solution. (c) The observation that the crystalline samples bind O_2 non-cooperatively was thus concluded to be proof that T tetramers in solution would also be devoid of cooperativity unless they followed an aberrant allosteric mechanism, i.e., with different rules from those of O_2-binding.

The above argument embodies the supposition that, if cooperative interactions had existed among subunits of the quaternary T tetramer in solution, they would somehow not have been suppressed in the crystal lattice and would have been observed. However, this supposition ignores the fact that the tertiary structure changes upon which any such cooperativity within T tetramers would necessarily depend (since heme centers remain 25–40 Å apart) have clearly been suppressed by the crystal lattices, as evidenced by the extraordinary reduction of bind-

ing affinity and by the complete absence of any (tertiary) Bohr effect [50,52,14]. The supposition that if cooperativity without quaternary switching occurs in solution it would also have been manifested under the additional crystalline constraints is therefore not credible. Although the crystal binding measurements of Mozzarelli and co-workers are technically fascinating, their relationship to solution properties is not clear.

The energetic magnitude of O_2 cooperativity for the path along species 01 → 11 → 21 was predicted in 1992 to be 2 kcal, compared with 3 kcal for both $Fe^{2+}/Fe^{2+}CN$ and Fe^{2+}/Mn^{3+} and 0.6 kcal for $Co^{2+}/Fe^{2+}CO$ [20]. Recently a value of 2 kcal has been determined for this cooperativity in the Zn^{2+}/FeO_2 system [11]. This value is nearly identical with the corresponding value for $Fe^{2+}/Fe^{2+}CO$ [10], all under identical solution conditions. Although it is expected that the different analog systems should have varying magnitudes of their cooperativity effects, a common set of mechanistic rules encoded in Eq. (14) accommodates all of these diverse systems.

2.6. Heterotropic ligands

Even though the mechanistic features summarized in the preceding sections have accounted for the flow of homotropic cooperativity through the cascade of 16 heme site reactions that connect the 10 ligation species (Fig. 1), it is also of foremost importance to deduce the coupling rules for heterotropic interactions with Bohr protons, chloride, DPG and CO_2. Recent work with CN-met microstates [14,15] has found two distinct Bohr proton linkages: (i) a *tertiary Bohr effect* in which proton release upon initial ligation of tetramers exceeds that of dissociated dimers; and (ii) a *quaternary Bohr effect*, in which additional proton release accompanies each T → R transition. These Bohr proton effects, which are synchronized with the two kinds of structural transition, were found to distribute through the reaction cascade in accord with symmetry rule predictions, i.e., proton release accompanied only the eight heme ligation steps that generated tertiary constraint or quaternary T → R transition, whereas the remaining eight reactions were found to have only the same proton linkages as dissociated dimers. A precisely identical specific ordering was found previously among the 16 cooperative enthalpies of the reaction cascade [16]. The finding of a tertiary Bohr effect using CN-met ligation is consistent with the earlier demonstration that proton release at the first O_2-binding step exceeds that of dissociated dimers [50].

A principal goal of the present work was to determine whether these characteristic "tertiary" and "quaternary" responses are also manifested for the heterotropic effects of NaCl. Does salt modulate the cooperative free energy distribution according to the same specific code found with cooperative free energies, enthalpies, and Bohr protons? What relationships exist between chloride-linked effects on cooperativity in the CN-met analog system and those of oxygen-binding? A parallel study of assembly-linked stoichiometric oxygen-binding over the same range of experimental conditions is presented in the paper by Doyle et al. [3]. Comparisons can thus be made between the results of this study on salt linkages of the 16 CN-met ligation reactions and the corresponding salt linkages at the four stages of stoichiometric O_2-binding.

3. Materials and methods

3.1. Preparation of hemoglobins

Purification of Hbs A_0 and S were carried out as described [25]. The purified proteins were stored in standard analytical buffer (0.1 M Tris, 0.1 M NaCl, 1 mM EDTA, pH 7.40 at 21.5°C) under liquid nitrogen. Samples were thawed in an ice bath prior to use. The standard buffer for these experiments varied in [NaCl] to give a range of 0.08–1.4 M total chloride. Buffer exchange of Hb samples was effected either by use of a G-25 Sephadex column equilibrated in the buffer or by Centricon 30 (Amicon) centrifugation exchange at 4°C.

CN-met Hb and CN-met α- or β-chains were prepared by adding excess of 1 M $K_3Fe(CN)_6$ for 5 min at room temperature. The KCN (10% molar excess) was added for an additional 5 min. CN-met Hb samples were run across a G-25 Sephadex column at 4°C to remove excess oxidant and to place the sample in the appropriate buffer. Hemoglobin species 23 and 24 were prepared by the method of Blough and Hoffman [26]. The purity of species 23

and 24 was verified using cryo- isoelectric focusing, which confirms that no excess of α- or β-chain is present in these samples.

3.2. Analytical gel chromatography (AGC)

Dimer–tetramer assembly free energies of species 23, 24, and 41 at different values of [NaCl] were determined by large zone experiments [27,28] performed in a Coy anaerobic chamber where the O_2 pressure was below 1 ppm. A Sephadex G-100 (Sigma) column with a bed volume slightly larger than 30 ml was maintained at 21.5°C by a circulating water jacket connected to a Lauda K-2/R bath (Brinkmann Instruments). Complete deoxygenation of the Sephadex column was achieved by continuously running the column with deoxygenated standard buffer for at least two days. Samples were prepared by placing the Hb under a flow of humidified N_2 for 1 h and then placing them in the anaerobic chamber. For species 23 and 24, an additional 20 min inside the oxygen-free chamber was required to insure full deoxygenation. The samples were maintained below 10°C while being slowly agitated on a shaker plate during deoxygenation. Each concentration of hemoglobin was achieved by diluting the sample with anaerobic standard analytical buffer to achieve a total volume of 20 ml. The sample was loaded onto the column with extreme care and the elution profiles were monitored using a Shimadzu UV-150-02 spectrophotometer. Plateau protein concentration was varied over the range 0.06–300 μM.

The weight-average partition coefficient $\bar{\sigma}_w$ of each Hb sample was evaluated from the determined centroid (equivalent sharp boundary) elution volumes (V_e) using the equation

$$\bar{\sigma}_w = \frac{V_e - V_0}{V_i} \tag{15}$$

where V_0 and V_i are the void and the internal volumes, respectively. V_i and V_0 were determined using glycylglycine and blue dextran in "small zone" experiments. The difference in peak elution positions ($V_{gly} - V_{dex}$) provided V_i for each column. For an interacting system of hemoglobin dimers the weight-average partition coefficient $\bar{\sigma}_w$ depends on the equilibrium fraction of dimers (f_D) and tetramers (f_T) in the plateau region of each large zone and their respective partition coefficients σ_D and σ_T [27,28]

$$\bar{\sigma}_w = \sigma_D f_D + \sigma_T f_T \tag{16}$$

The fraction of dimer f_D is a function of the equilibrium constant for dimer–tetramer assembly K_2 and the total hemoglobin concentration P_t as follows

$$f_D = \frac{-1 + \sqrt{1 + 4K_2 P_t}}{2K_2 P_t} \tag{17}$$

Data of $\bar{\sigma}_w$ versus P_t were fitted to simultaneous Eq. (16) and Eq. (17) using a nonlinear least-squares program, NONLIN [29], to resolve the equilibrium constant K_2.

At each [NaCl], three or more zones were obtained for each species with plateau concentrations that varied by at least 10-fold. Elution volumes were determined as the centroid values of both leading and trailing boundaries [27]. These values were transformed into weight-average partition coefficients using the void and internal volumes (Eq. (15)).

To obtain valid equilibrium constants of dimer–tetramer assembly, it is important to ensure that the distribution of the dimers and tetramers are in pseudo-equilibrium during chromatography. In our measurements, sensitivity in elution volume is within 1% (about 0.02 ml) of the difference in V_e between dimer and tetramer. For a typical flow rate of 15 ml h^{-1}, the sensitivity range corresponds to a time scale of 5 s. The dissociation rate constants for species 41, 23, and 24 in 0.18 M chloride were previously evaluated to be in the range 0.6–1.5 s^{-1}, corresponding to half-times of 1.1 to 0.5 s. These are well below the sensitivity range, indicating that the assembly reactions are in a pseudo-equilibrium state in these experiments. In addition, however, the observed constancy of plateau concentrations requires by conservation of mass alone that $\bar{\sigma}_w$ reflects the true equilibrium for the plateau concentration [27].

3.3. Hybridization experiments

Six species (i.e., 11, 12, 21, 22, 31, and 32) were studied in hybrid mixtures with their corresponding

parent species, as indicated in Fig. 2. When the parent species are mixed, their dissociation into dimers which reassemble in proportion to their hybridization free energies yields tetramers with rearranged configurations of ligated sites. Sample mixing was performed under anaerobic conditions within a N_2 glove bag. *Aspergillus niger* catalase (0.3 mg ml^{-1}), glucose oxidase (1.8 mg ml^{-1}), and glucose (0.6%) were added to insure full deoxygenation. After mixing, the samples were aliquoted and placed in large rubber-sealed vials containing fresh 0.1% sodium dithionite solution to eliminate oxygen contamination during incubation (cf. [6]). This step has been found crucial for incubations longer than ≈ 12 h [6]. Then the aliquots were placed in a temperature-controlled water bath until they were quenched at -30°C. The quench buffer contained a 1:1 ratio of ethylene glycol and standard analytical buffer. After quenching, the Hb sample was saturated with CO to prevent oxidation of the ferrous hemes and then loaded into cryo-isoelectric focusing gel tubes. Each sample was focused overnight at -25°C, yielding three distinct bands (see [6] for tests of equilibration). Relative populations of the three tetrameric species in the hybrid mixture were determined by spectrophotometric scanning of the gel and integration of the respective profiles [6]. Activity of the enzyme system was found to decrease substantially at 1.4 M chloride. To achieve full deoxygenation, Hb samples were first mixed with the enzyme system for 10 min at low [NaCl] (0.18 M). Then a high-concentration NaCl solution was added to the samples to give a final concentration of 1.4 M. Finally the Hb samples were mixed to initiate hybrid formation. The sample at 1.4 M chloride was quenched into buffer at -30°C containing 0.18 M chloride to avoid interference with electrophores by the high salt concentration. To verify the absence of significant re-equilibrium of a hybrid mixture during the electrophoresis at -25°C, controls were carried out by quenching two parent species separately at -30°C. The samples were then mixed and loaded into IEF tubes for 24 hours of focusing at -25°C. Less than 2% of hybrid species was found in these experiments, indicating no significant dissociation of the parent tetramer.

Quantitation of the three populations yielded equilibrium fractions (f_{AA}, f_{BB} and f_{AB}) for the respective tetrameric species in a hybrid mixture, and the deviation free energy δ was then calculated

$$\delta = -RT \ln \frac{f_{AB}}{2\sqrt{f_{AA} f_{BB}}} \tag{18}$$

where parent species AA and BB have dissociated and reassembled their dimeric halves to form the hybrid AB [6]. Using independently determined assembly free energies of the parent species, the free energy ${}^{AB}\Delta G_2$ of assembling the hybrid is determined

$$\delta = {}^{AB}\Delta G_2 - \frac{1}{2}\left({}^{AA}\Delta G_2 + {}^{BB}\Delta G_2\right) \tag{19}$$

4. Experimental results

4.1. Assembly free energies of species 23, 24 and 41

Weight-average partition coefficients are plotted in Fig. 3 versus the "large zone" plateau concentrations for species 41 at [NaCl] values ranging from 0.08 to 1.4 M. Determination of the equilibrium

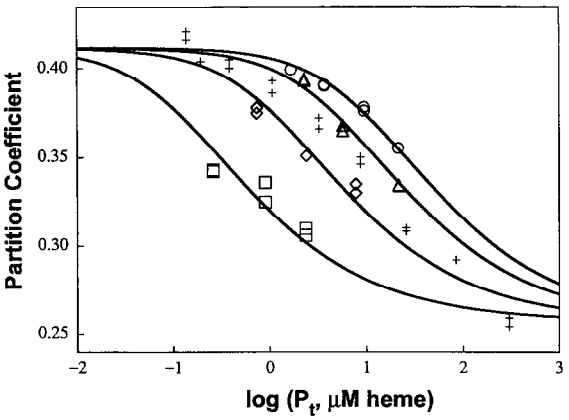

Fig. 3. Weight-average partition coefficients versus Hb concentrations from "large zone" analytical gel chromatography. Data for cyanomet Hb were determined at NaCl concentrations of 0.08 M (□), 0.35 M (◇), 0.70 M (△), and 1.4 M (○). Results shown are from both the leading and the trailing boundaries of each elution profile. Curves represent best-fit parameters from global analysis of parameters for the respective dimer–tetramer equilibria of cyanomet Hb. Data for oxy-Hb (+) determined at 0.35 M chloride are included for comparison. Other solution conditions: 0.1 M Tris, 1 mM EDTA, 10 μM KCN, pH 7.40 and 21.5°C.

constants by Eqs. (16) and (17) required the asymptotic partition coefficients pertaining to pure dimeric and tetrameric species. To obtain these "end-state" parameters, experiments were conducted with oxy-Hb over a 1000-fold range of plateau concentrations. The resulting weight-average partition coefficients $\bar{\sigma}_w$ for oxy-Hb and those for species 23, 24 or 41 were fitted simultaneously to Eq. (16) to estimate the dimeric and tetrameric partition coefficients. Confidence intervals obtained for each resolved equilibrium constant thus included the uncertainty from "floating" $\bar{\sigma}_D$ and $\bar{\sigma}_T$ during analysis. Fig. 3 shows curves representing the best-fit parameters for assembly of species 41. Data for oxy-Hb at 0.35 M chloride are also shown for comparison. Assembly free energies for oxy-Hb determined by the AGC method are in good agreement with those determined by stopped flow kinetics [3] as shown in Table 1. Chloride dependences of the assembly free energies for species 23, 24 and 41 are plotted in Fig. 4.

At high values of [NaCl], i.e. 0.7 M and 1.4 M, the elution profiles for species 23 and 24 showed slightly uneven plateaus and slight inconsistency between centroids for the leading and trailing boundaries of each zone, suggesting minor heterogeneity of the samples. This unusual behavior appeared to result from exposing the deoxygenated protein to high-salt buffer. We attempted to deoxygenate species 23 and 24 at high concentration (1–3 mM) in low chloride (0.18 M) and then diluted them with buffers containing high chloride. Samples were immediately loaded onto the column for the AGC experiment. This procedure substantially reduced the time of exposure of the proteins to high-salt buffer and resulted in flat plateaus for both species at 0.7 M chloride. However, slight inconsistency between centroids of the leading and trailing boundaries of these zones remained at 0.7 and 1.4 M chloride concentrations. Free energies pertaining to high [NaCl] were therefore estimated using only data from the leading boundaries, where protein had the shortest exposure to high-salt buffer. Estimated errors of assembly free energy at 0.7 and 1.4 M chloride (0.3–0.4 kcal) were slightly higher than the typical error (0.2 kcal) found at lower [NaCl].

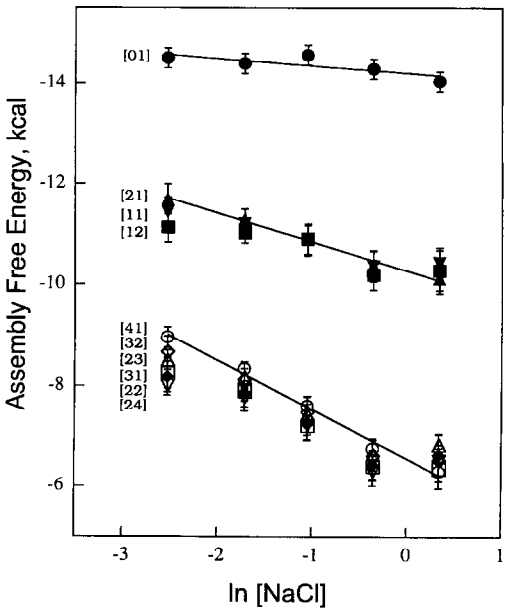

Fig. 4. Assembly free energies of the 10 ligation species versus logarithm of NaCl concentration. Species 01 (●), 11 (▼), 12 (■), 21 (▲), 22 (◆), 23 (△), 24 (▼), 31 (□), 32 (◆), and 41 (○). Curves are linear representations of the data for species 01, 21 and 41. Solution conditions as in Fig. 3.

Table 1
Comparison of assembly free energies for oxy-hemoglobin determined by analytical gel chromatography and by stopped flow kinetics

[NaCl]/M	Analytical gel chromatography	Stopped flow [a]
0.08	−8.67±0.30	−8.55±0.10
0.18	−8.07±0.10	−8.05±0.10
0.35	−7.16±0.27	−7.30±0.10
0.70	−6.57±0.10	−6.40±0.10

[a] Equilibrium constants are from amplitude analysis of dimer–tetramer assembly reactions initiated by rapid deoxygenation (cf. Doyle et al., 1997).

4.2. Assembly free energies of hybrid species

It was necessary to study these species in hybrid mixture with their respective parent tetramers (see Fig. 2). Assembly free energies were accordingly calculated by Eqs. (18) and (19). Equilibrium fractions of each hybrid and its two parents were determined using quantitative cryogenic isoelectric focusing [6]. The approach to equilibrium in forming

hybrid species was monitored by determining fractions of each tetramer in the mixture versus hybrid incubation time. Equilibration time for species 11 or 12 was 20–30 h and that for species 21 was 75–100 h. The quality of species separation and baseline integrity was comparable with that presented earlier [6,18]. No significant changes in kinetics of hybrid formation were found with changing chloride concentration within the range 0.08–1.4 M chloride. Equilibration times for species 22, 31 and 32 were found to be short (i.e., minutes) at each chloride concentration employed. Deviation free energies (δ) were evaluated from the equilibrium population data using Eq. (4). For all six hybrid species these values were found in the range 0.0–0.2 kcal within the chloride concentration range. Assembly free energies of the hybrids were calculated by Eq. (19) using their measured deviation free energies and the ${}^{ij}\Delta G_2$ values of the parental species 23, 24, and 41 as found by AGC determinations, and also with the assembly free energy previously determined for species 01 [3].

Standard Gibbs energies, ${}^{ij}\Delta G_2$, of dimer–tetramer assembly for all ten ligation microstates are summarized in Fig. 4 at the chloride concentrations of this study. Assembly energies for species 01 showed little dependence on chloride concentration, in agreement with earlier work [30]. However, ${}^{ij}\Delta G_2$ values of the nine ligated species were found to become less negative with increasing [NaCl], indicating that increasing concentrations of chloride promote tetramer disassembly. The actual dependence of ${}^{ij}\Delta G_2$ on [NaCl] is specific for the number of hemes ligated and their site configurations, with species 41 showing the largest dependence.

4.3. Combinatorial distributions vs. [NaCl]

Assembly free energies and cooperative free energies of the ten CN-met ligation species have previously been found to distribute into three distinct levels according to a combinatorial feature, i.e., dependence both on the number of ligands bound and on the configuration of ligated subunits for a given number bound (see [44] for a recent review). The doubly ligated species are found in two of these free energy levels, with species 21 behaving differently from the other three (i.e., species 22, 23, and 24). An objective in the present study was to investigate whether this combinatorial distribution of cooperative free energies for the ten ligation species is robust with respect to changing chloride concentration.

The distributions found in this study (Fig. 4) exhibit the same characteristic combinatorial distribution among cooperative free energies for the 10 ligation species at each NaCl concentration studied. Characteristic features of the distribution remain invariant, whereas energetic spacings between the levels increase with decreasing [NaCl]. This characteristic distribution (Eqs. (10)–(13)) among terms of the partition function, as resolved on model-independent grounds, has also been found at pH values ranging from 7.0 to 9.5 [14] and at temperatures from 5°C to 26°C [16]. Resolution of the chloride linkages carried out in this study adds an important step in elucidating the roles of heterotropic effectors at the level of tertiary and quaternary responses. The present study, in combination with those cited above, leads to the conclusion that symmetry rule behavior is manifested for both the homotropic and the heterotropic modulation of heme site binding in CN-met Hb. This implies that the fundamental structure changes (tertiary and quarternary) that accompany the changes in combinational site occupancy also exert tight control over the interactions with heterotropic ligands.

4.4. Linkages to chloride release

To estimate the apparent changes in bound chloride (${}^{ij}\Delta\bar{\nu}_2$) upon assembly, the data of Fig. 4 were fitted to the following linkage relationship

$$\frac{-\mathrm{d}\,{}^{ij}\Delta G_2}{RT\,\mathrm{d}(\ln a_{\mathrm{NaCl}})} = {}^{ij}\Delta\bar{\nu}_2 \qquad (20)$$

where ${}^{ij}\Delta G_2$ is the dimer–tetramer assembly free energy of species ij, R is the gas constant and T is the temperature. Thermodynamic activities of NaCl (a_{NaCl}) were calculated at each concentration using activity coefficients from Weast [31]. Each data point was weighted according to the standard deviation of ${}^{ij}\Delta G_2$. For partially ligated species (except species 21), dependences of ${}^{ij}\Delta G_2$ on ln[NaCl] were found to deviate from linearity only above 0.7 M chloride.

The origin of such deviations is not clear, and changes in apparent moles of bound chloride upon assembly ${}^{ij}\Delta\bar{\nu}_2$ were evaluated using data within the [NaCl] range 0.08–0.7 M. The resulting values for all ten species are given in Table 2. The negative sign for ${}^{ij}\Delta\bar{\nu}_2$ indicates chloride release.

The dimer–tetramer assembly reactions of deoxy-Hb (species 01) and of each microstate species ij are thermodynamically linked to the respective ligand-binding reactions [2] as shown by the scheme of Eq. (21)

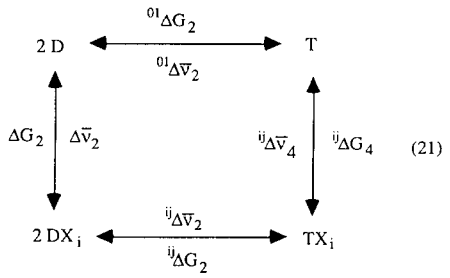

The chloride-linked component of each tetrameric ligation, relative to its constituent dimers (${}^{ij}\Delta\bar{\nu}_c = {}^{ij}\Delta\bar{\nu}_4 - \Delta\bar{\nu}_2$) is equal to the differential change of bound chloride (${}^{ij}\Delta\bar{\nu}_c$) upon assembly of species ij relative to that of unligated species 01 (${}^{01}\Delta\bar{\nu}_2$)

$$ {}^{ij}\Delta\bar{\nu}_c = {}^{ij}\Delta\bar{\nu}_2 - {}^{01}\Delta\bar{\nu}_2 \qquad (22) $$

The determined values of ${}^{ij}\Delta\bar{\nu}_c$ are given in Table 2.

It should be noted that these calculations of ${}^{ij}\Delta\bar{\nu}_2$ and ${}^{ij}\Delta\bar{\nu}_c$ ignore the effect of changing water chemical potential caused by the presence of high salt concentration. Studies by Colombo et al. [32,33] have indicated that part of the apparent chloride release upon oxygenation of Hb may be due to the perturbation of water activity by the presence of high [NaCl]. They estimated that approximately 65 molecules of thermodynamically bound water were released upon full oxygenation. Reciprocally then, changes in the chemical potential of water might result in perturbation of the oxygen-binding. A recent study of chloride release upon heme site ligation and subunit assembly [51] has controlled the thermodynamic activity of water with compensating sucrose while varying the chemical potential of NaCl. These determinations showed that the combinatorial distribution found in the present study of the 10 ligation species of CN-met Hb was equally clearcut, and thus not a resultant of compensating effects that mask a more fundamental distribution. A similar issue with respect to the contributions to cooperative free energies by enthalpic and entropic terms has been addressed earlier [16].

Table 2
Apparent change in moles of bound chloride ($\Delta\bar{\nu}_{Cl}$) accompanying dimer–tetramer assembly of partially ligated tetramers [a]

Species	Assembly ${}^{ij}\Delta\nu_2$ [a]	Ligation ${}^{ij}\Delta\nu_c$ [b]
Cyanomet species		
01	−0.23±0.20	−0
11	−0.99±0.16	−0.76
12	−0.90±0.35	−0.67
21	−1.04±0.20	−0.81
22	−1.65±0.27	−1.42
23	−1.76±0.27	−1.53
24	−1.62±0.37	−1.39
31	−1.65±0.22	−1.42
32	−1.84±0.16	−1.61
41	−1.83±0.15	−1.60
Oxy-Hb		
41	−1.87±0.15	−1.64

[a] Tetramers minus their constituent dimers (scheme in Eq. (21)).
[b] The ${}^{ij}\Delta\nu_c$ values were calculated from ${}^{ij}\Delta\nu_2$ data using Eq. (22).

4.5. Overall oxygen binding and cyanomet ligation

Cooperative oxygen-binding by Hb has long been known to be modulated by chloride. The "chloride effect" is generally considered to arise from specific chloride-binding events, general ionic strength effects, and, at high concentration, alteration of water activity [32–35]. Most researchers have utilized NaCl rather than KCl to study these effects, even though potassium ion is the physiologically abundant species in the red cell. No specific binding sites that would prefer K^+ have been identified in studies with KCl (e.g., [36–39]). These studies have shown functional effects with KCl similar to those with NaCl. It should be noted, however, that the strongest binding

occurs at concentrations below 0.05 M salt [36–39], which is below the range of most studies including the present one. Comparative studies on NaCl vs. KCl should be carried out in the lower concentration regime as an extension of the present work. An X-ray crystal structure showed an O_2-linked chloride-binding site at the val 1 position of the α subunits [40]. More recent studies showed that the magnitude of the chloride effect for a series of mutants (using NaCl) varied according to the number (0–4) of positive charges in the central cavity [41–43]. It would be of interest to resolve these effects at the more detailed level of the ten ligation microstates. However, the central issues of the present study are (a) whether the cyanomet ligation system generates similar responses to [NaCl] as those which accompany oxygen-binding over the commonly accessible range of most studies to date, and (b) whether the NaCl linkages to the 16 stepwise reactions of heme site binding are synchronized according to the molecule's tertiary and quaternary switches, as may be anticipated by the corresponding study of Bohr proton release [14].

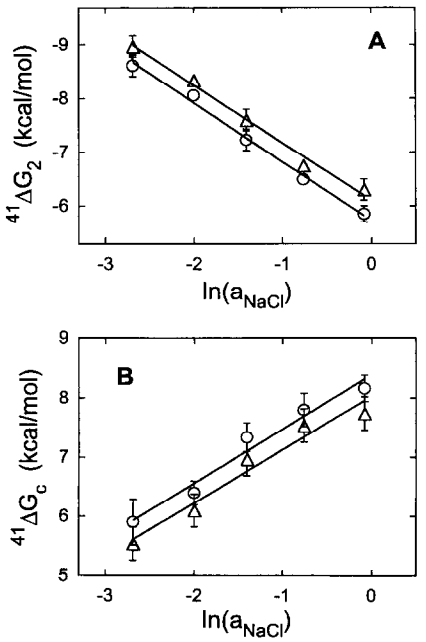

Fig. 5. Linkages between thermodynamic activities of NaCl and assembly free energies. A: Dimer–tetramer assembly free energies for oxy-Hb (○) and cyanomet Hb (△) versus logarithm of NaCl activity [i.e. chemical potential/($-RT$)]. B: Total cooperative free energies over all binding steps for ligand binding to Hb oxygen (○) and cyanomet (△). Values are plotted versus logarithm of NaCl activity. Lines depict linear least-squares fits.

Comparisons of interest between the O_2 and CN-met systems thus include the chloride dependences of assembly free energy for fully ligated Hb (Fig. 5A) and of the total cooperative free energy, i.e., over all binding steps (Fig. 5B). Cooperative free energies were calculated at each chloride concentration as the difference between assembly energies of fully liganded and unliganded Hb, Fig. 1. It was found that the effects on $^{41}\Delta G_2$ and $^{41}\Delta G_c$ of changing chloride concentration are identical for the two ligands (Fig. 5). Using linear fits of the data in Fig. 5A for oxy-Hb to obtain a slope for use in Eq. (20), the apparent number of moles of chloride linked to assembly was evaluated. The corresponding change in moles of chloride linked to ligation was then calculated from Eq. (22). These results are given in Table 2, where it is seen that $^{41}\Delta\bar{\nu}_2$ and $^{41}\Delta\bar{\nu}_c$ values for oxy-Hb are identical to the corresponding $^{41}\Delta\bar{\nu}_2$ and $^{41}\Delta\bar{\nu}_c$ values for cyanomet Hb. The excellent agreement between the two ligation systems (Fig. 5 and Table 2) indicates that overall modulation of cyanomet ligation by NaCl is identical to that for oxygen-binding.

5. Discussion

5.1. Correspondence with the symmetry rule mechanism

The present study on allosteric chloride effects is unprecedented in providing an experimental resolution of this classic heterotropic regulation at the level of each stepwise ligation reaction. The data in Table 2 indicate that there are two distinct chloride effects. (i) Approximately half of the total chloride release by tetramers (relative to dissociated dimers) is synchronized with the first heme site binding event. As the singly ligated cyanomet species 11 and 12 maintain the quaternary T interface [13–16,18–22], it follows that the first chloride effect is coupled to the tertiary structural changes that are induced upon initial ligation of the tetramer. Detailed structural origins of this tertiary chloride effect may include

ligand-induced alterations of salt bridges within solvent-accessible regions of the tetrameric structure and conformational strain that perturbs interactions between ionizable groups and chloride ions. (ii) The second component of ligation-linked chloride release is seen from this study to be manifested at each of the six switchpoints of quaternary T → R transition which are specified by the symmetry rule. Thus the same molecular code that translates the configuration-specific ligation states into tertiary and quaternary structural changes also prescribes the rules of heterotropic salt linkage. A precisely similar finding was established recently for tertiary and quaternary Bohr proton release in CN-met Hb [14], including the finding that the overall Bohr effect has identical magnitude for CN-met and O_2 ligation.

5.2. Origins of the allosteric salt effects

X-ray diffraction studies on deoxy- and oxy-Hb have shown that a network of salt bridges and hydrogen bonds is present within the $\alpha^1\beta^2$ interface of deoxy-Hb. Upon binding oxygen these bonds are broken and a quaternary transition takes place. For example, the salt bridges across the $\alpha^1\beta^2$ interface of deoxy-Hb have long been suggested to play an important role in governing the quaternary transition [45]. Since these salt bridges are also formed during dimer–tetramer assembly, studying the effects of "competing salt" on their assembly reactions would be expected to provide useful mechanistic constraints. Other studies of the effects of salt on assembly free energy of deoxy-Hb and oxy-Hb ([3,30]) showed that increasing [NaCl] had little effect on the ΔG_2 of deoxy-Hb, but it substantially reduced the negative free energy of dimer–tetramer assembly. This study has also found that assembly free energy for cyanomet Hb is much less negative in the presence of higher [NaCl] (Fig. 4). These results might be viewed as contradictory to an oversimplified concept that the effect of competing salt on assembly of deoxy-Hb should be greater than that on fully ligated Hb, since there are more salt bridges in the dimer–dimer interface of deoxy-Hb. However, other types of interactions are also of importance to tetrameric stability. The recent findings of Perutz et al. [42] also suggest that the $\alpha^1\beta^2$ interfacial salt bridges may not be the sole source of the allosteric chloride effects.

5.3. Relationships between CN-met microstate properties and the intermediates of O_2-binding

It is of particular interest to compare the present results on salt linkages of the CN-met microstate species with those from the parallel study [3] of stoichiometric O_2-binding linkages to dimer–tetramer assembly over an identical range of [NaCl]. In that study a large salt-dependent quaternary enhancement effect was observed at the fourth oxygen-binding step, whereas quaternary enhancement in the CN-met species has been only marginally detectable (cf. [14]). For purposes of comparison we note that, for any ligand, the stoichiometric coupling constants ${}^iK_c$ (corrected for statistical factors) are each comprised of the microstate parameters ${}^{ij}k_c$ according to relationships Eqs. (23)–(26), which are model-independent.

$$2({}^1K_c) = {}^{11}k_c + {}^{12}k_c \tag{23}$$

$${}^1K_c = K_{tc} \tag{23a}$$

$$6({}^2K_c) = 2({}^{21}k_c) + 2({}^{22}k_c) + {}^{23}k_c + {}^{24}k_c \tag{24}$$

$$3({}^2K_c) = K_{tc}^{21} + 2K_cK'_{tc} \tag{24a}$$

$$2({}^3K_c) = {}^{31}k_c + {}^{32}k_c \tag{25}$$

$${}^3K_c = K_cK'_{tc} \tag{25a}$$

$${}^4K_c = {}^{41}k_c \equiv K_c \tag{26}$$

Translation into parameters of the symmetry rule mechanism is accomplished by substituting from Eqs. (10)–(13) to obtain relationships Eqs. (23a), (24a) and (25a) and the rightmost equivalence of Eq. (26). Each of these relationships constrains one of the experimental coupling constants ${}^iK_c$ in relation to parameters of the molecular code partition function, Eq. (14). Eqs. (25a), (24a) and (23a) readily permit evaluation of K'_{tc}, K_{tc}^{21} and K_{tc} from the data at each concentration of NaCl, while K_c is known on model-independent grounds.

For comparison between experimental assembly free energies of the two data bases (O_2 and CN-met), all terms in these equations may be multiplied by the

respective ${}^{01}k_2$ values (or ${}^{01}K_2$ in the stoichiometric nomenclature), and then converted into assembly free energies using

$$ {}^{ij}\Delta G_2 = -RT \ln\left[\left({}^{ij}k_c\right)\left({}^{01}k_2\right)\right] \quad (27) $$

The resulting distribution, plotted against NaCl concentration for the O_2 data in Fig. 6, may be compared with those of Fig. 5 for the CN-met system. The range and overall variation with [NaCl] of the asembly free energies for species 41 are essentially identical for the two ligands, as noted earlier. At the lowest [NaCl] the values for singly ligated species 11 and 12 are also essentially identical. However, the CN-met system shows a greater variation with increasing [NaCl] than does the O_2 system. Thus a larger tertiary chloride effect is found with CN-met species 11 and 12 than for singly-O_2 Hb. From values in Table 2, the tertiary chloride effect Δv_c is approximately -0.7 mol, as compared with -0.3 mol for singly oxygenated Hb [3]. Notably, the CN-met system shows negligible quaternary enhancement over the entire [NaCl] range, whereas the O_2 system exhibits a large effect that is titrated by NaCl. This is seen in Fig. 6 by the comparison between data for species 41 and the triply ligated species 31 and 32.

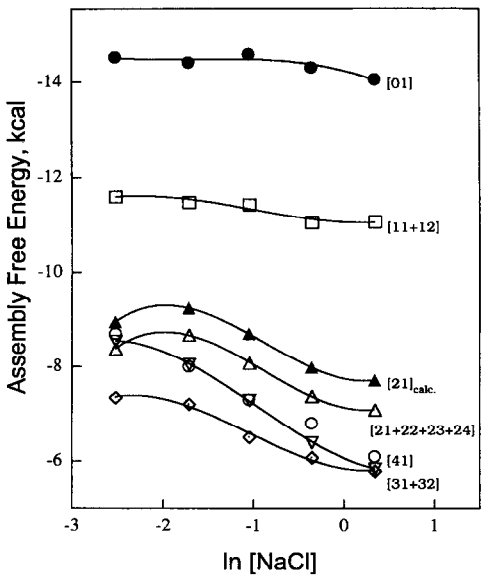

Fig. 6. Salt dependences of assembly free energies for human hemoglobin with various combinations of bound O_2. Experimental values (Doyle et al., accompanying manuscript) are plotted for tetramers: (●) unligated; (□) singly oxygenated; (▲, △) doubly oxygenated; (◇) triply oxygenated; (▽) triply CN-met ligated and (○) fully oxygenated. The configurational isomers *ij* within each binding stoichiometry are given in brackets. (s) Assembly free energies for the asymmetric doubly ligated species 21, evaluated at each [NaCl] by Eq. (24).

Although the Hb structural transitions that accompany quaternary enhancement are not yet understood, the crystallographic finding of a third quaternary structure designated "Y" or R2 for fully ligated hemoglobins [46–48] suggests the possibility that quaternary equilibria may play a role in solution at the final steps of binding after switchover from the T structure has occurred. Assuming that the crystallized molecular structures also reflect the characteristic solution quaternary structures under given salt conditions, it has been suggested that increasing salt favors R over R2 for molecules that are triply or fully oxygenated (cf. [3]). Then the large quaternary enhancement found in low [NaCl] for O_2 and its observed titration by salt may reflect a predominence of Y/R2 tetramers contributing to the species 41 assembly free energies of Fig. 6 at low [NaCl], and an enhanced proportion of quaternary R molecules promoted by increasing salt concentration. The triply oxygenated species titration curve (shown as 31 + 32 in Fig. 6) would reflect essentially the salt dependence of dimer–tetramer assembly for quaternary R tetramers. This ordering of salt titration curves for triply and fully oxygenated Hb would also correspond with findings on the mutant Hb Ypsilanti [48], which exhibits large quaternary enhancement and crystallizes as Y/R2 tetramers when fully oxygenated [46]. The finding in this study that assembly free energy of CN-met species 41 has a salt dependence very similar to that of O_2-Hb species [42], but very different from that of triply oxygenated Hb, is also consistent with the recent crystallographic finding of Smith and Simmons [49] that CN-met species 41 has a quaternary Y/R2 structure at low salt (i.e. 0.18 M). These consistencies between the crystal structures and solution properties suggest that CN-met species 41 may remain in the Y/R2 structure at all [NaCl] conditions of the present study. If the common species 41 profile in Figs. 4 and 6 is characteristic of quaternary Y/R2, it follows that CN-met species 22, 23, 24, 31, and 32 may also

adopt this form. Evaluation of these possibilities will require additional structural analyses. The symmetry rule partition function, Eq. (11), could accommodate either a quaternary or a tertiary transition (or an equilibrating mixture of both) at the final binding step.

Acknowledgements

This program of research has greatly benefited during the past 10 years from the numerous discussions and suggestions by participants of the annual Gibbs Conference on Biological Thermodynamics.

Supported by NSF GRANT DMB9405492, and by NIH Grants R37GM24486 and PO1-HL51084.

References

[1] F.R. Smith and G.K. Ackers, Proc. Natl. Acad. Sci. U.S.A., 82 (1985) 5347.
[2] G.K. Ackers and F.R. Smith, Annu. Rev. Biophys. Biophys. Chem., 16 (1987) 583.
[3] M.L. Doyle et al., Biophys. Chem., 64 (1997).
[4] M. Perrella, L. Benazzi, M.A. Shea and G.K. Ackers, Biophys. Chem., 35 (1990) 97.
[5] M. Perrella, A. Colosimo, L. Benazzi, M. Ripamonti and L. Rossi-Bernardi, Biophys. Chem., 37 (1990) 211.
[6] V.J. LiCata, P.C. Speros, E. Rovida and G.K. Ackers, Biochemistry, 29 (1990) 9772.
[7] F.R. Smith, D. Gingrich, B.M. Hoffman and G.K. Ackers, Proc. Natl. Acad. Sci. U.S.A., (1987).
[8] P.C. Speros, V.J. LiCata, T. Yonetani and G.K. Ackers, Biochemistry, 30 (1991) 7254.
[9] M.L. Doyle, P.C. Speros, V.J. LiCata, D. Gingrich, B.M. Hoffman and G.K. Ackers, Biochemistry, 30 (1991) 7263.
[10] Y. Huang and G.K. Ackers, Biochemistry, 35 (1996) 704.
[11] Y. Huang, M.L. Doyle and G.K. Ackers, Biophys. J., 71 (1996) 2094.
[12] G.K. Ackers and H.R. Halvorson, Proc. Natl. Acad. Sci. U.S.A., 71 (1974) 4312.
[13] M.L. Doyle and G.K. Ackers, Biochemistry, 31 (1992) 11182.
[14] M.A. Daugherty, M.A. Shea and G.K. Ackers, Biochemistry, 33 (1994) 10345.
[15] M. Perrella, Biochemistry, 33 (1994) 10358.
[16] Y. Huang and G.K. Ackers, Biochemistry, 34 (1995) 6316.
[17] G.K. Ackers, Biophys. Chem., 37 (1990) 371.
[18] M.A. Daugherty, M.A. Shea, J.A. Johnson, V.J. LiCata, G. Turner and G.K. Ackers, Proc. Natl. Acad. Sci. U.S.A., 88 (1991) 1110.
[19] V.J. LiCata, P.M. Dalessio and G.K. Ackers, Proteins, 17 (1993) 279.
[20] G.K. Ackers, M.L. Doyle, D. Myers and M.A. Daugherty, Science, 255 (1992) 54.
[21] E. Di Cera, Thermodynamic Theory of Site-Specific Binding Processes in Biological Macromolecules, Cambridge University Press, 1995.
[22] V. Jayaraman, K.R. Rodgers, I. Mukerji and T.G. Spiro, Science, 269 (1993) 1843.
[23] J. Monod, J. Wyman and J.-P. Changeux, J. Mol. Biol., 12 (1965) 88.
[24] D.E. Koshland, G. Nemethy and D. Filmer, Biochemistry, 5 (1966) 365.
[25] R.C. Williams and K.Y. Tsay, Anal. Biochem., 54 (1973) 137.
[26] N.V. Blough and B.M. Hoffman, Biochemistry, 23 (1984) 2875.
[27] G.K. Ackers, Adv. Protein Chem., 24 (1970) 343.
[28] R. Valdes, Jr., and G.K. Ackers, Methods Enzymol., 51 (1979) 125.
[29] M.L. Johnson and S.G. Frasier, Methods Enzymol., 117 (1985) 301.
[30] A.H. Chu and G.K. Ackers, J. Biol. Chem., 256 (1981) 1199.
[31] R.C. Weast, CRC Handbook of Chemistry and Physics, 53rd edn., The Chemical Rubber Company, 1972, p. D-123.
[32] M.F. Colombo, D.C. Rau and V.A. Parsegian, Science, 256 (1992) 655.
[33] M.F. Colombo, D.C. Rau and V.A. Parsegian, Proc. Natl. Acad. Sci. U.S.A., 91 (1994) 10517.
[34] R.N. Haire and B.E. Hedlund, Proc. Natl. Acad. Sci. U.S.A., 74 (1977) 4135.
[35] K. Imaizumi, K. Imai and I. Tyuma, J. Biochem., 86 (1979) 1829.
[36] S.H. de Bruin, H.S. Rollema, H.M. Lambert and G.A.J. Van Os, Biochem. Biophys. Res. Commun., 58 (1974) 210.
[37] H.S. Rollema, S.H. de Bruin, L.H.M. Janssen and G.A.J. Van Os, J. Biol. Chem., 250 (1975) 1333.
[38] G.M. Van Beek, E.R.P. Zuiderweg and S.H. de Bruin, Eur. J. Biochem., 99 (1979) 379.
[39] G.M. Van Beek and S.H. de Bruin, Eur. J. Biochem., 105 (1980) 353.
[40] S. O'Donnell, R. Mandaro, T.M. Schuster and A. Arnone, J. Biol. Chem., 254 (1979) 12204.
[41] H. Ueno and J.M. Manning, J. Protein Chem., 11 (1992) 177.
[42] M.F. Perutz, D.T. Shih and D. Williamson, J. Mol. Biol., 239 (1994) 555.
[43] C. Bonaventura, M. Arumugam, R. Cashon, J. Bonaventura and W.J. Moo-Penn, J. Mol. Biol., 239 (1994) 561.
[44] J. Holt and G.K. Ackers, FASEB J., 9 (1995) 210.
[45] M.F. Perutz, Nature, 228 (1970) 734.
[46] F.R. Smith, E.E. Lattman and C.W. Carter, Proteins, 10 (1991) 81.
[47] M.M. Silva, P.H. Rogers and A. Arnone, J. Biol. Chem., 267 (1992) 17248.
[48] M.L. Doyle, G. Lew, G.J. Turner, D.L. Rucknagel and G.K. Ackers, Proteins, 14 (1992) 351.

[49] F.R. Smith and K.C. Simmons, Proteins, 18 (1994) 597.
[50] A.W.M. Lee, M. Karplus, C. Poyart and E. Bursaux, Biochemistry, 27 (1088) 1285.
[51] Y. Huang, M.L. Koestner and G.K. Ackers, Biophys. J., 71 (1996) 2106.
[52] A. Mozzarelli, C. Rivetti, G.L. Rossi, E.R. Henry and W.A. Eaton, Nature, 351 (1991) 416.
[53] C. Rivetti, A. Mozzarelli, G.L. Rossi, E.R. Henry and W.A. Eaton, Biochemistry, 32 (1993) 2888.
[54] S. Bettati, A. Mozzarelli, G.L. Rossi, A. Tsuneshige, T. Yonetani, W.A. Eaton and E.R. Henry, Proteins, 25 (1996) 425.